Linear Scaling of the Exciton Binding Energy versus the Band Gap of Two-Dimensional Materials

Jin-Ho Choi, Ping Cui, Haiping Lan, and Zhenyu Zhang

Phys. Rev. Lett. **115**, 066403 — Published 7 August 2015

DOI: 10.1103/PhysRevLett.115.066403

Linear scaling of the exciton binding energy versus the band gap of two-dimensional materials

Jin-Ho Choi,[1,2] Ping Cui,[1,2] Haiping Lan,[1] and Zhenyu Zhang[1,2]

[1]*International Center for Quantum Design of Functional Materials (ICQD), Hefei National Laboratory for Physical Sciences at the Microscale, University of Science and Technology of China, Hefei, Anhui 230026, China*

[2]*Synergetic Innovation Center of Quantum Information and Quantum Physics, University of Science and Technology of China, Hefei, Anhui 230026, China*

ABSTRACT

Exciton is one of the most crucial physical entities in the performance of optoelectronic and photonic devices, and widely varying exciton binding energies have been reported in different classes of materials. Using first-principles calculations within the *GW*-Bethe-Salpeter equation approach, here we investigate the excitonic properties of two recently discovered layered materials, phosphorene and graphene fluoride. We first confirm large exciton binding energies of respective 0.85 eV and 2.03 eV in these systems. Next, by comparing these systems with several other representative two-dimensional materials, we discover a striking linear relationship between the exciton binding energy and the band gap, and interpret the existence of the linear scaling law within a simple hydrogenic picture. The broad applicability of this novel scaling law is further demonstrated using strained graphene fluoride. These findings are expected to stimulate related studies in higher and lower dimensions, potentially resulting in a deeper understanding of excitonic effects in materials of all dimensionalities.

PACS numbers: 71.35.−y, 73.22.−f, 78.67.−n

An exciton is a pair of electron and hole mutually bound together by an attractive electrostatic force, and is also one of the most important physical quantities in designing different kinds of optoelectronic, photonic, and catalytic devices [1-4]. The precise binding energy of an exciton, given by the amount of energy required to separate an excitonic electron-hole pair, is a key measure of excitonic effects within a given system. It is thus highly desirable to determine accurately the exciton binding energies of various materials.

In three-dimensional (3D) systems such as bulk semiconductors, the exciton binding energies are typically only a few tens of meV, indicating weakly bound excitons due to effective electronic screening. In systems of reduced dimensionalities, the electronic screening is less effective, potentially resulting in more strongly bound excitons. Indeed, the exciton binding energies of several 1D and 2D materials [5-7] are at least an order of magnitude larger than those of bulk semiconductors, making excitonic effects more pronounced. In retrospect, each time a new and significant low-D material was discovered, its corresponding excitonic behavior would be routinely exploited on a timely manner, using state-of-the-art computational and experimental approaches. Successful examples in the 2D cases include a hexagonal BN sheet [6], graphane [8], monolayered MoS_2 [9], and the special case of semi-metallic graphene [10], using first-principles calculations within the *GW*-Bethe-Salpeter equation (*GW*-BSE) approach [11-14]. Results from such state-of-the-art studies are also expected to stimulate related experimental explorations.

In this Letter, we first use the *GW*-BSE approach to investigate the excitonic properties of two recently discovered 2D materials, phosphorene [15,16] and graphene fluoride [17,18]. Our results show that both systems have direct quasi-particle (QP) band gaps, given by 2.26 eV and 7.70 eV for phosphorene and graphene

fluoride, respectively; the corresponding exciton binding energies are 0.85 eV and 2.03 eV, confirming that both of the layered materials possess strongly bound excitons as expected or reported recently [19-22]. More importantly, by putting these two systems into a collective perspective with several representative 2D systems, we discover a striking linear relationship between the exciton binding energy and the QP band gap, whose underlying physical reason is further revealed within a simple hydrogenic model. Using strained graphene fluoride as an example, we also demonstrate the broad applicability of the novel scaling law to many existing and future 2D materials. These findings will stimulate related studies in higher- and lower-dimensional materials, potentially resulting in a deeper understanding of excitonic effects in materials of all dimensionalities.

The density functional theory calculations [23] were carried out using the projector-augmented wave method [24,25] and the Perdew-Wang (PW91) [26] exchange correlation functional as implemented in the Vienna *ab-initio* simulation package [27]. The energy cutoff for the plane-wave basis set is 400 eV. All atoms are allowed to fully relax until the forces exerted on each atom are less than 0.02 eV/Å. The optimized atomic structures [Figs. 1(a) and 1(b)] within the PW91 scheme are used in the following *GW*-BSE calculations: the obtained lattice parameters are a = 4.63 Å, b = 3.32 Å for phosphorene, and a = b = 2.60 Å for graphene fluoride. The *GW* calculations were performed in a partially self-consistent way (the so-called GW_0 approach) [14]. For both phosphorene and graphene fluoride, two self-consistent updates for the Green's function (the G_2W_0 approach) were sufficient to converge the QP band gap to within 10 meV. The energy cutoff for the response functions was set to be 266.7 eV, and the obtained band gap is essentially the same if a higher cutoff of 333.3 eV is used. To plot the QP band structures, we use the approach of maximally

localized Wannier functions [28]. The corresponding optical gap was obtained by solving the BSE on top of the *GW* results. The BSE calculations were performed using the ten highest valence bands and ten lowest conduction bands of each system.

In order to obtain the accurate QP band gaps, it is vital to carefully examine the convergence of the QP bands in the *GW* calculations. In a recent *GW* study, the QP bands of ZnO were shown to converge very slowly with the number of unoccupied bands included [29]. The slow convergence is attributed to the existence of highly localized states characterized by relatively flat bands [29]. Fortunately, phosphorene and graphene fluoride possess no such highly localized bands, and the QP band gaps converge rapidly with respect to the number of unoccupied bands. Specifically, 181 and 182 unoccupied bands are sufficient for graphene fluoride and phosphorene, respectively. Due to long-range Coulomb interactions, the spatial separation L_z between the 2D sheets needs to be examined for convergence as well [6,30,31]. Figures 1(c) and 1(d) show the dependence of the QP band gap on the inverse spatial separation for phosphorene and graphene fluoride, respectively. Here, we use 11×15×1 and 15×15×1 *k*-point meshes for each system, which are also tested for the convergence of the *GW*-BSE calculations. Since the QP band gap converges as $1/L_z$ [30,32], we extrapolate the gaps to the limit of infinite L_z. The extrapolated band gaps are in close agreement with those from the Coulomb truncation scheme [31] within ~0.1 eV, as discussed in the Supplemental Material [33]. For both systems, L_z of 30 Å provides well-converged QP band gaps, while the optical gap is already well converged with L_z of only 10 Å. The QP band structures and optical absorption spectra were all obtained with L_z = 30 Å. More details about the convergence tests are given in the Supplemental Material [33].

We first investigate the electronic and optical properties of phosphorene using the

GW-BSE approach. As seen in Fig. 2(a), phosphorene is a relatively wide-gap semiconductor with a direct gap at the Γ point. The QP band gap obtained by extrapolation is 2.26 eV. The effective masses of electron and hole can be estimated by fitting the QP bands to the parabolic form of $E(k) = \frac{\hbar^2 k^2}{2m^*}$. The estimated electron effective masses are highly anisotropic, given by 0.46 m_e in the armchair direction [along **x** in Fig. 1(a)] and 1.12 m_e in the zigzag direction [along **y** in Fig. 1(a)], where m_e is the electron rest mass. The corresponding hole effective masses are also highly anisotropic, given by 0.23 m_e and 1.61 m_e along the **x** and **y** direction, respectively.

Figure 2(b) shows the calculated optical absorption spectrum of phosphorene for light polarized along the armchair direction. The optical gap is 1.43 eV, indicated by the first peak of the absorption spectrum. The first peak along the zigzag direction is located at 3.31 eV (not shown). By extrapolating to the limit of infinite L_z, we obtain the optical gap of 1.41 eV, which agrees well with the experimental value of 1.45 eV [16]. The corresponding exciton binding energy defined by the energy difference between the QP band gap and the optical gap is 0.85 eV, confirming strongly bound excitons in such a 2D material. The exciton binding energy obtained here is very close to that (~0.8 eV) reported in a recent *GW*-BSE study [19].

We next investigate the electronic and optical properties of graphene fluoride. Here, we consider only the chair configuration [Fig. 1(b)], which is the most stable structure of graphene fluoride [34]. We find that graphene fluoride has a direct band gap at the Γ point [Fig. 3(a)], which is extrapolated to be 7.70 eV. We note that the QP band gap is considerably larger than that (7.49 eV) obtained by a similar GW_0 approach [35]. This difference is likely caused by the smaller spatial separation L_z employed in the previous *GW* calculation (15 Å), which is insufficient to converge the QP bands as clearly seen in Fig. 1(d). The estimated effective masses are isotropic,

given by 0.61 m_e and 0.58 m_e for electron and hole, respectively. A detailed analysis of the projected densities of states (PDOS) on the constituent atoms reveals that both the valence band maximum (VBM) and conduction band minimum (CBM) are fairly evenly distributed on the C and F atoms: 53% on C and 47% on F for the VBM, and 49% on C and 51% on F for the CBM. The calculated optical absorption spectrum for graphene fluoride is displayed in Fig. 3(b). The optical gap is 5.67 eV, consistent with the values of 5.4 eV ~ 5.6 eV from two previous *GW*-BSE studies [20,21]. These values are much higher than the lower limit of ~3.8 eV measured in a recent experiment [18], while a separate *GW*-BSE study reported almost the same optical gap as experimentally observed [22]. As discussed previously [20,21,34], the discrepancy in the optical gap between theory and experiment could be ascribed to the effects of corrugation and defects in the graphene fluoride samples, which may create mid-gap states, effectively narrowing the optical gap. The corresponding exciton binding energy is 2.03 eV, indicating even more strongly bound excitons in this wider band-gap 2D material.

Next we explore the relationship between the exciton binding energy and the QP band gap, by putting the present results of phosphorene and graphene fluoride into a collective perspective with the previous findings of other representative 2D materials such as graphane, monolayered MoS_2 [9], SiC and BN sheets. Here the convergence issue of exciton binding energy has been more distinctly recognized only recently, we have repeated most of the calculations for such systems (including the previously studied ones), but with mutually comparable higher accuracy. It is worthwhile to emphasize that, whereas graphane and a SiC sheet both possess direct band gaps, a BN sheet has an indirect band gap, as indicated in Figs. S3-S5 of the Supplemental Material [33]. More detailed *GW*-BSE results for the other 2D materials are given in

the Supplemental Material [33]. In Fig. 4, we display the binding energies (E_b) and the band gaps (E_g) of those 2D materials. Strikingly, the data establish a well-defined linear dependence, given by $E_b = \alpha E_g + \beta$, with $\alpha = 0.21$ and $\beta = 0.40$. Figure 4 suggests that, when the QP band gap is below 0.5 eV, the exciton binding energy could be larger than the band gap in such 2D systems, even implying the possible existence of excitonic effects in 2D or quasi-2D metals due to incomplete or non-instantaneous screening [36]. In this regime, various scattering mechanisms of excitons with other degrees of freedom are also expected to play more important roles in leading to exciton relaxation, an intriguing aspect beyond the scope of the present study. These data were drawn from both strongly anisotropic and isotropic example systems, yet they all obey the same scaling law. Qualitatively, larger band gaps imply weaker screening, which in turn should lead to stronger binding within an electron-hole pair. The scaling relationship is qualitatively consistent with this expectation, but precisely why in 2D it should be linear is conceptually challenging.

We can examine the applicability of the linear scaling relation in severely strained 2D systems, as mechanical strain is often applied in tuning the band gap and the corresponding electronic and optical properties of materials [37]. Here, we have carried out *GW*-BSE calculations for 10% tensile-strained graphene fluoride, with a = b = 2.87 Å. The calculated QP band gap and optical gap are 6.72 eV and 4.92 eV, respectively, and the corresponding exciton binding energy is 1.80 eV. The binding energy and the band gap again show an excellent agreement with the linear scaling law, as highlighted in Fig. 4. Given the wide ranges of both the band gaps and the exciton binding energies represented in Fig. 4, and the different classes of systems (isotropic or strongly anisotropic), we have a strong basis to expect that the linear scaling relation is applicable to essentially all existing and future 2D materials.

Here we propose a first-order model interpretation of the linear scaling law. According to the hydrogenic model, the exciton binding energy E_b of 2D quantum well systems is linearly proportional to μ/ε^2, where μ is the reduced mass, and ε is the dielectric constant [38]. Because the dielectric constants of 2D layered systems with infinitesimal thickness are essentially the same as the vacuum dielectric constant [39], we have $\varepsilon = 1$ and $E_b \propto \mu$ for such 2D systems. Separately, within the $k \cdot p$ perturbation theory, the effective masses of electron and hole are approximately proportional to the band gap E_g with particle-hole symmetry [40], which in turn leads to $E_b \propto \mu \propto E_g$. Here we note that even if particle-hole symmetry is broken, μ can still be proportional to E_g as long as both the electron and hole effective masses are proportional to E_g. It should also be noted that, even though the present explanation is based on a very simplified model, it does capture the central aspects of the linear scaling relation, and is expected to stimulate further efforts on developing more sophisticated model interpretations.

With the establishment of the linear scaling law between the exciton binding energy and the corresponding band gap in 2D materials, it is also natural to search for possible existence of similar scaling laws in other dimensions. For 3D systems, extensive experimental results suggest the existence of an exponential or higher-order powered relationship between the exciton binding energy and the band gap [41], even though such a relationship has not been explicitly emphasized previously. On the other hand, we expect a weaker than linear scaling dependence in 1D systems. This trend is indeed qualitatively supported by the limited examples in previous *GW*-BSE studies of carbon and BN nanotubes [5,6]. We also note the prediction and experimental confirmation of power law dependences between the exciton binding

energy of carbon nanotubes and the tube radius or dielectric constant of the surrounding media [42,43]. These intriguing aspects are to be explored systematically in future studies.

In summary, we have used the state-of-the-art *GW*-BSE approach and a diverse range of example systems to establish a well-defined and striking linear scaling law between the exciton binding energies and QP band gaps of 2D materials. The underlying physical reason of the linear scaling law has been further revealed within a simple hydrogenic model based on the $k \cdot p$ perturbation theory. The broad applicability of this novel scaling law has also been demonstrated using strained graphene fluoride. We expect that the present work will stimulate related studies in higher and lower dimensional systems, potentially resulting in a deeper understanding of excitonic effects in systems of all dimensionalities.

Acknowledgements: J.-H. C. and P. C. contributed equally to this work. We thank Profs. Steven G. Louie and Mei-Yin Chou for their encouraging comments on the validity of the linear scaling law. We are particularly grateful to Prof. Erio Tosatti for an insightful suggestion on the hydrogenic model. This work was supported in part by the National Natural Science Foundation of China (Nos. 61434002, 11350110325, 11204286), the Chinese Academy of Sciences Fellowships for Young International Scientists (2011Y2JB10), National Research Foundation of Korea (2012R1A6A3A03040199), and National Key Basic Research Program of China (2014CB921103). Part of the calculations was carried out at the National Energy Research Scientific Computing Center, which is supported by the Office of Science of the U. S. Department of Energy under Contract No. DE-AC02-05CH11231.

Note added - After the submission of this paper, we become aware of two very recent experimental studies of the exciton binding energies in monolayered $MoSe_2$ and WS_2 [44-45]. In particular, after properly correcting substrate effects, both the experimentally observed and the *GW*-BSE calculated exciton binding energies of $MoSe_2$ [44] are sufficiently consistent with the expectation of the linear scaling law shown in Fig. 4.

References

1. Y. Sun, N. C. Giebink, H. Kanno, B. Ma, M. E. Thompson, and S. R. Forrest, Nature **440**, 908 (2006).
2. X. F. Duan, Y. Huang, Y. Cui, J. F. Wang, and C. M. Lieber, Nature **409**, 66 (2001).
3. D. Stich, F. Späth, H. Kraus, A. Sperlich, V. Dyakonov, and T. Hertel, Nat. Photon. **8**, 139 (2013).
4. Y. Miyauchi, M. Iwamura, S. Mouri, T. Kawazoe, M. Ohtsu, and K. Matsuda, Nat. Photon. **7**, 715 (2013).
5. C. D. Spataru, S. Ismail-Beigi, L. X. Benedict, and S. G. Louie, Phys. Rev. Lett. **92**, 077402 (2004).
6. L. Wirtz, A. Marini, and A. Rubio, Phys. Rev. Lett. **96**, 126104 (2006).
7. H. C. Hsueh, G. Y. Guo, and S. G. Louie, Phys. Rev. B **84**, 085404 (2011).
8. P. Cudazzo, C. Attaccalite, I. V. Tokatly, and A. Rubio, Phys. Rev. Lett. **104**, 226804 (2010).
9. D. Y. Qiu, F. H. da Jornada, and S. G. Louie, Phys. Rev. Lett. **111**, 216805 (2013).
10. L. Yang, Phys. Rev. B **83**, 085405 (2011).
11. S. Albrecht, L. Reining, R. Del Sole, and G. Onida, Phys. Rev. Lett. **80**, 4510 (1998).
12. L. X. Benedict, E. L. Shirley, and R. B. Bohn, Phys. Rev. Lett. **80**, 4514 (1998).
13. M. Rohlfing and S. G. Louie, Phys. Rev. Lett. **81**, 2312 (1998).
14. G. Onida, L. Reining, and A. Rubio, Rev. Mod. Phys. **74**, 601(2002).
15. L. Li, Y. Yu, G. J. Ye, Q. Ge, X. Ou, H. Wu, D. Feng, X. H. Chen, and Y. Zhang, Nat. Nanotechnol. **9**, 372 (2014).

16. H. Liu, A. T. Neal, Z. Zhu, Z. Luo, X. Xu, D. Tománek, and P. D. Ye, ACS Nano **8**, 4033 (2014).
17. J. T. Robinson, J. S. Burgess, C. E. Junkermeier, S. C. Badescu, T. L. Reinecke, F. K. Perkins, M. K. Zalalutdniov, J. W. Baldwin, J. C. Culbertson, P. E. Sheehan, and E. S. Snow, Nano Lett. **10**, 3001 (2010).
18. K.-J. Jeon, Z. Lee, E. Pollak, L. Moreschini, A. Bostwick, C.-M. Park, R. Mendelsberg, V. Radmilovic, R. Kostecki, T. J. Richardson, and E. Rotenberg, ACS Nano **5**, 1042 (2011).
19. V. Tran, R. Soklaski, Y. Liang, and L. Yang, Phys. Rev. B **89**, 235319 (2014).
20. D. K. Samarakoon, Z. Chen, C. Nicolas, and X.-Q. Wang, Small **7**, 965 (2011).
21. F. Karlický and M. Otyepka, J. Chem. Theory Comput. **9**, 4155 (2013).
22. Y. Liang and L. Yang, MRS Proceedings **1370**, 137 (2011).
23. W. Kohn and L. J. Sham, Phys. Rev. **140**, A1133 (1965).
24. P. E. Blöchl, Phys. Rev. B **50**, 17953 (1994).
25. G. Kresse and D. Joubert, Phys. Rev. B **59**, 1758 (1999).
26. J. P. Perdew, J. A. Chevary, S. H. Vosko, K. A. Jackson, M. R. Pederson, D. J. Singh, and C. Fiolhais, Phys. Rev. B **46**, 6671 (1992).
27. G. Kresse and J. Furthmüller, Phys. Rev. B **54**, 11169 (1996); Comput. Mater. Sci. **6**, 15 (1996).
28. A. A. Mostofi, J. R. Yates, Y.-S. Lee, I. Souza, D. Vanderbilt, and N. Marzari, Comput. Phys. Commun. **178**, 685 (2008).
29. B.-C. Shih, Y. Xue, P. Zhang, M. L. Cohen, and S. G. Louie, Phys. Rev. Lett. **105**, 146401 (2010).
30. N. Berseneva, A. Gulans, A. V. Krasheninnikov, and R. M. Nieminen, Phys. Rev. B **87**, 035404 (2013).

31. S. Ismail-Beigi, Phys. Rev. B **73**, 233103 (2006).

32. J. P. A. Charlesworth, R. W. Godby, and R. J. Needs, Phys. Rev. Lett. **70**, 1685 (1993).

33. See Supplemental Material for more details of the convergence tests in the *GW*-BSE calculations and the band structures and the absorption spectra of the other 2D materials, which includes Refs. [19,20,30-32].

34. O. Leenaerts, H. Peelaers, A. D. Hernández-Nieves, B. Partoens, and F. M. Peeters, Phys. Rev. B **82**, 195436 (2010).

35. H. Şahin, M. Topsakal, and S. Ciraci, Phys. Rev. B **83**, 115432 (2011).

36. X. Cui, C. Wang, A. Argondizzo, S. Garrett-Roe, B. Gumhalter, and H. Petek, Nat. Phys. 10, 505 (2014).

37. E. D. Minot, Y. Yaish, V. Sazonova, J.-Y. Park, M. Brink, and P. L. McEuen, Phys. Rev. Lett. **90**, 156401 (2003).

38. P. Harrison, *Quantum Wells, Wires and Dots*, 2nd ed. (Wiley, Chichester, 2005), p. 203.

39. P. Cudazzo, I. V. Tokatly, and A. Rubio, Phys. Rev. B. **84**, 085406 (2011).

40. R. Winkler, *Spin-Orbit Coupling Effects in Two-Dimensional Electron and Hole Systems* (Springer, Berlin, 2003), p. 12.

41. H. Haug and S. W. Koch, *Quantum Theory of the Optical and Electronic Properties of Semiconductors*, 4th ed. (World Scientific Publ., Singapore, 2004), p. 176.

42. V. Perebeinos, J. Tersoff, and P. Avouris, Phys. Rev. Lett. **92**, 257402 (2004).

43. A. G. Walsh, A. N. Vamivakas, Y. Yin, S. B. Cronin, M. S. Ünlü, B. B. Goldberg, and A. K. Swan, Nano Lett. **7**, 1485 (2007).

44. M. M. Ugeda, A. J. Bradley, S.-F. Shi, F. H. da Jornada, Y. Zhang, D. Y. Qiu, W. Ruan, S.-K. Mo, Z. Hussain, Z.-X. Shen, F. Wang, S. G. Louie, and M. F. Crommie, Nat. Mater. **13**, 1091 (2014).

45. B. Zhu, X. Chen, and X. Cui, Sci. Rep. **5**, 9218 (2015).

Figure Captions

Figure 1. (color online). Side (upper panel) and top view (lower panel) of (a) phosphorene and (b) graphene fluoride. Each unit cell is indicated by the solid lines. (c) and (d): The QP band gap as a function of the inverse spatial separation $1/L_z$ for phosphorene and graphene fluoride, respectively. In (c) and (d), the dots indicate the results of the G_0W_0, G_2W_0, and BSE calculations, while the dashed lines represent the corresponding extrapolations.

Figure 2. (a) Calculated QP band structure and (b) optical absorption spectrum of phosphorene. The absorption spectrum for incident light along the armchair direction. In (a), the zero energy is set to the valence band maximum. In (b), the positions of the first absorption peak and the QP band gap are denoted by the dotted line and the arrow, respectively.

Figure 3. (a) Calculated QP band structure and (b) optical absorption spectrum of graphene fluoride.

Figure 4. The exciton binding energy (E_b) versus the QP band gap (E_g) for various representative 2D materials. The dashed line represents the fitted linear relation in the form of $E_b = \alpha E_g + \beta$, with $\alpha = 0.21$ and $\beta = 0.40$. The fitted data are denoted by the filled symbols, while the unfilled data point for strained graphene fluoride helps to demonstrate the broad applicability of the scaling relationship.

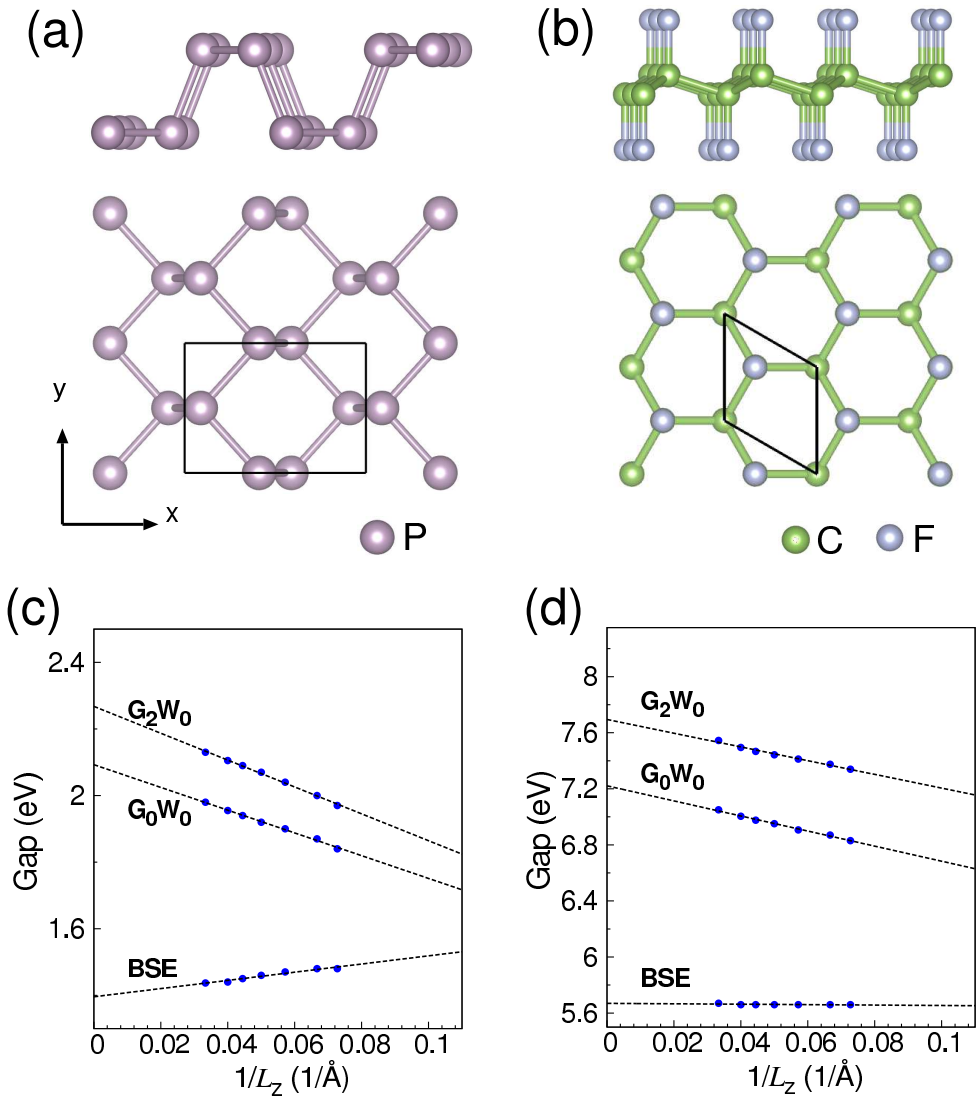

Figure 1 LV13833 15JUL2015

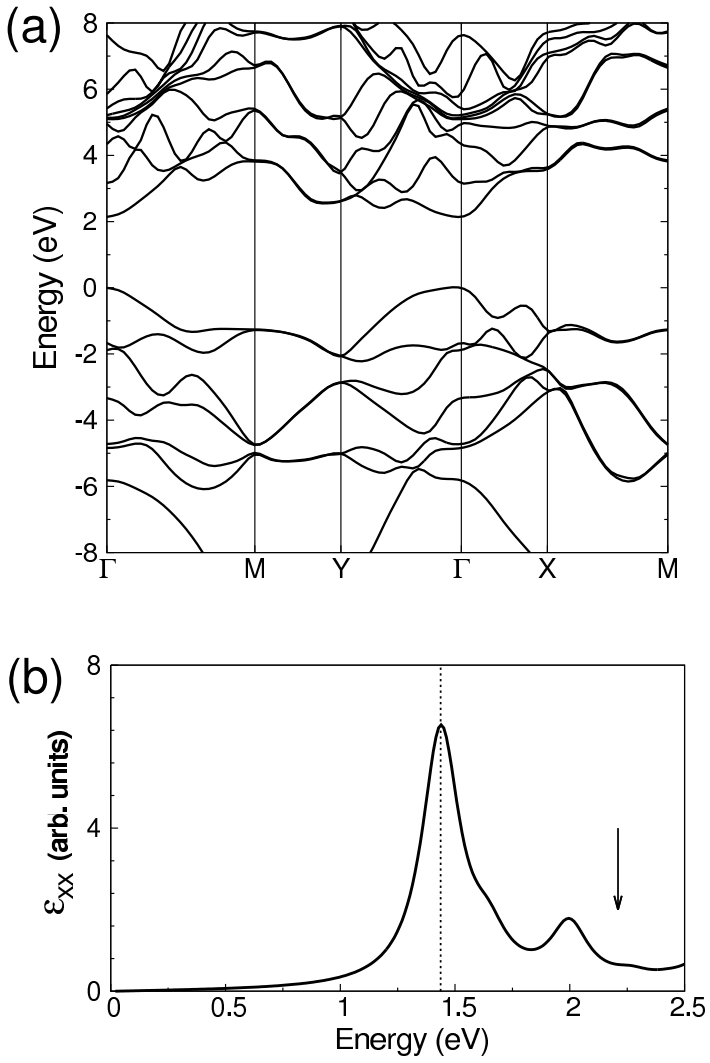

Figure 2 LV13833 15JUL2015

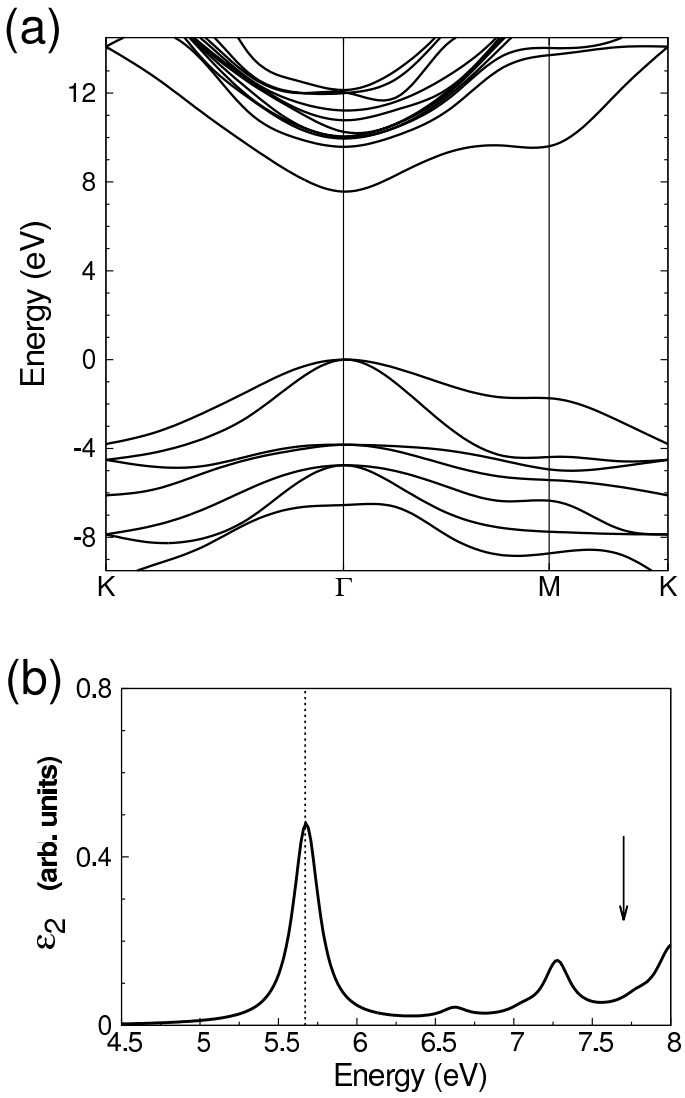

Figure 3 LV13833 15JUL2015

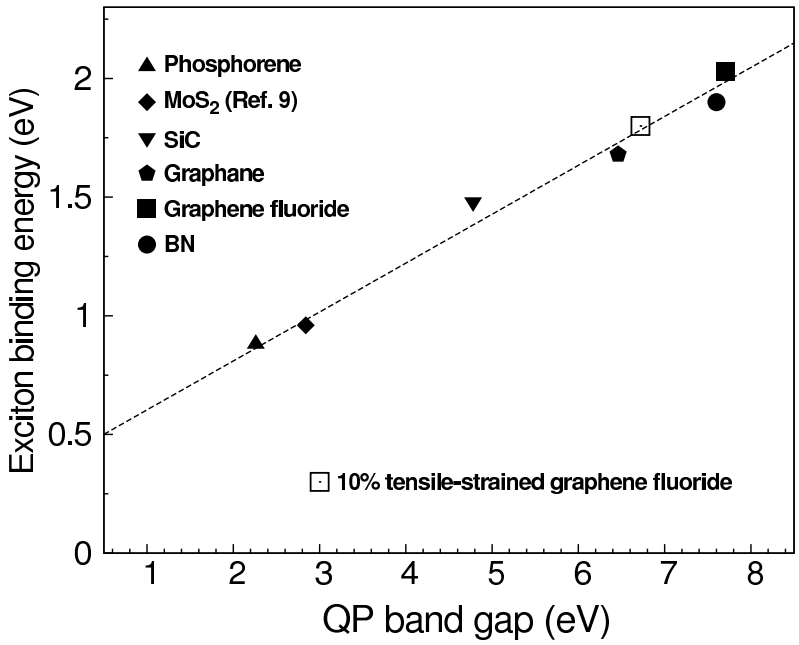

Figure 4 LV13833 15JUL2015